Classical and quantum optical correlation effects between single quantum dots: The role of the hopping photon

S. Hughes*
Department of Physics, Queen's University, Kingston, Ontario, Canada K7L 3N6

H. Gotoh and H. Kamada
NTT Basic Research Laboratories, NTT Corporation, 3-1 Morinosato-Wakamiya, Atsugi, Kanagawa 243-0198, Japan
(Received 13 January 2006; published 29 September 2006)

We present a theoretical study of photon-coupled single quantum dots in a semiconductor. A series of optical effects are demonstrated, including a subradiant dark resonance, superradiance, reversible spontaneous emission decay, and pronounced exciton entanglement. Both classical and quantum optical approaches are presented using a self-consistent formalism that treats real and virtual photon exchange on an equal footing and can account for different quantum dot properties, surface effects, and retardation in the dipole-dipole coupling, all of which are shown to play a non-negligible role.

DOI: 10.1103/PhysRevB.74.115334 PACS number(s): 78.67.Hc, 42.25.Bs, 42.50.−p, 42.55.Tv

I. INTRODUCTION

Nanoscale confinement of both photons and charge carriers is now possible, thereby facilitating new and exciting light-matter interaction regimes. In this regard optical studies of single quantum dots (QDs) are of broad interest both from a fundamental physics viewpoint and also because of their applications potential in scalable single-photon applications.[1–3] Single QDs also show promise in the area of optically addressed qubit control because of their two-level quantum behavior,[4] large optical dipole moments, and long optical dephasing times.[4–6]

The resonant exchange of photons by identical and closely spaced atoms has been studied for quite some time.[7–9] Atoms can become photon coupled when they are placed very close to each other, leading to dipole-dipole interactions and the Förster exchange process. Such effects are well established in the field of atomic optics, and can also be enhanced considerably by modifying the photonic vacuum, e.g., by embedding the coupled atoms in a high-Q cavity[10] and (or) a photonic band gap.[11] From a practical point of view, the exploitation and realization of useful photonic devices more suitable to optical wavelengths would more likely be realized in the solid state optics domain. However, in the field of quantum confined semiconductor systems, which have substantially larger and in general different dipole moments (and resonance energies), the influence on single-QD spectroscopy and spontaneous emission dynamics is still largely unknown or neglected, since single QDs by definition are usually assumed well separated from neighboring QDs, so that their optical properties are determined only by the measurement and analysis of the single QD alone. Recently, evidence of photon exchange has been observed for two closely stacked self-assembled InAs/GaAs dots,[12] though since the QDs were very close together the role of electronic tunneling needs further investigation. So some clearer guidelines as to the expected influence of photon coupling for nearby QDs is desired, especially for distances where electronic tunneling cannot play any role.

In this work we introduce a general methodology to theoretically investigate the influence of photon-exchange coupling from neighboring QDs, in the linear optical regime, and show that it can be a significant effect when analyzing the optical properties of individual QDs. Our results imply that dipole interactions can also be useful especially for QDs that are close together, but still far enough apart that their coupling lies outside the regime of electronic tunneling. We approach this problem by using a photon Green function formalism that allows one to obtain an analytical expression for the permittivity for two coupled QDs (with dimensions much smaller than a wavelength), and to have a straightforward numerical solution for the quantum decay dynamics for an arbitrary number of coupled dots. Real and virtual photon transitions are treated on an equal footing. Although the equations extend naturally to many QDs, we specialize our analysis here to two coupled QDs since their spatial separation would be practically much easier to systematically control, e.g., via vertical stacking; the general theoretical treatment, however, can be applied to both vertical or laterally coupled QDs. The analysis and definition of exciton *entanglement* also takes on a precise meaning when we consider the coupling dynamics between two excitonic qubits (quantum bits), and this quantum regime is accessible using experimental techniques currently employed in single-QD spectroscopy.

II. THE SELF-CONSISTENT CLASSICAL APPROACH

One can write out the solution for the classical electric field as

$$\mathbf{E}(\mathbf{r};\omega) = \mathbf{E}^b(\mathbf{r};\omega) + \int d\mathbf{r}' \overleftrightarrow{\mathbf{G}}^b(\mathbf{r},\mathbf{r}';\omega) \cdot \Delta\epsilon_d(\mathbf{r}',\omega)\mathbf{E}(\mathbf{r}';\omega) \tag{1}$$

where $\overleftrightarrow{\mathbf{G}}^b$ is the background Green's function tensor (GFT), which describes the field response at $\mathbf{r}'$ to an oscillating dipole at $\mathbf{r}$, as a function of frequency, and $\mathbf{E}^b(\mathbf{r};\omega)$ is the solution prior to adding the electric permittivity perturbation $\Delta\epsilon_d$. The QD permittivity properties can then be added self-

consistently to obtain the new fields. Without any QD, the homogeneous GFT is known analytically.[13] One has

$$\overleftrightarrow{\mathbf{G}}^b(\mathbf{r},\mathbf{r}';\omega)=\frac{e^{ik_bR}k_b}{4\pi R\epsilon_b}\left(\overleftrightarrow{\mathbf{1}}+\frac{ik_bR-1}{(k_bR)^2}\overleftrightarrow{\mathbf{1}}+\frac{3-3ik_bR-k_b^2R^2}{(k_bR)^4}\mathbf{RR}\right) \tag{2}$$

where $R=|\mathbf{r}-\mathbf{r}'|$ and $k_b=\epsilon_b\omega^2/c^2$; ϵ_b is the background material relative permittivity. To include the influence of the surface, e.g., the capping layer of the QDs, one can obtain the exact GFT for a multilayer structure[14] that then includes effects due to the dielectric/air interface. The renormalized GFT (i.e., one that includes radiative coupling) can then be obtained self-consistently by exploiting the Dyson equation, which can be written, in operator form, as $\mathbf{G}=\mathbf{G}^b+\mathbf{G}^b\cdot\Delta\epsilon_d\cdot\mathbf{G}$, where $\mathbf{G}$ now includes the response of the QD. We assume a single QD with a volume V_d and diameter much smaller than the wavelength of light; thus the QD permittivity $\Delta\epsilon_d(\omega)=|\mathbf{d}|^2/[2V_d\epsilon_0\hbar(\omega_d-\omega-i\Gamma_d)]$, with $\mathbf{d}$ the electron-hole pair (exciton) dipole moment, Γ_d the nonradiative decay time of the QD, and ω_d the QD resonance frequency. In order to clarify the essential physics on two clearly coupled electron-hole pairs only the fundamental $1s$ exciton resonance is considered. A more detailed analysis of the various energy levels that may be involved including spin-Förster coupling is given by Goverov.[15] For one of the dots, QD a, the renormalized solution is simple to derive from the above; for an excitation field polarized in direction i, we have $\Delta\epsilon_a^{r1}(\omega)=\Delta\epsilon_a(\omega)/\{1-V_a\Delta\epsilon_a\,\mathrm{Im}[\mathbf{G}_{ii}^b(r_a,r_a;\omega)]\}$, where we neglect the small radiative shift (or it can be added into a renormalized ω_d); the superscript "$r1$" labels renormalization in the presence of one QD. Carrying out this procedure iteratively for two QDs a and b, one can derive the analytic permittivity expression for QD a (and similarly for b):

$$\Delta\epsilon_a^{r2}(\omega)=\frac{\Delta\epsilon_a^{r1}(\omega)+V_b\overleftrightarrow{\mathbf{G}}^b(r_a,r_b;\omega)\Delta\epsilon_a^{r1}(\omega)\Delta\epsilon_b^{r1}(\omega)E_b^0/E_a^0}{1-V_b\Delta\epsilon_b^{r1}(\omega)\overleftrightarrow{\mathbf{G}}^b(r_a,r_b;\omega)\Delta\epsilon_a^{r1}(\omega)\overleftrightarrow{\mathbf{G}}^b(r_b,r_a;\omega)V_a} \tag{3}$$

where E_α^0 ($\alpha=a,b$) is the externally excited field on QD α, r_a and r_b label (within the GFT) the spatial positions of the QDs, and "$r2$" represents the renormalized solution for two photon-coupled QDs; similar classical expressions have also been derived by Thomas *et al.*[16] The solution apparently depends on whether the system is excited with one or two resonant photons (thus E_b^0 would be on or off), and both cases are renormalized in different ways. The QDs can also be different and thus offer a broad range of coupling regimes.

We comment that recently a somewhat similar classical approach has been reported by Parascandola and Savona,[17] who also solve a self-consistent GFT problem to analyze long-range interaction effects between QDs including nonlocal contributions from the dots. Some interesting conclusions were reported, namely, that radiative coupling from nearby dots must typically be included when analyzing the general response of one QD, since interaction effects may persist even from QDs that are even quite far away; though, in general, such effects were rather small. We naturally recover such regimes, though present here a simpler formalism to enable analytical results to be obtained for two QDs within the GFT classical approach; and then we go on primarily to study the full quantum dynamics for QDs that are close together so as to explore and exploit photon exchange in a highly nonperturbative regime. We remark, further, that treating the QDs as point dipoles, as we do, has been shown to be an excellent approximation.[18] Thus, given that one rarely knows the exact dipole moments and QD shapes, unless they are taken from experiment, our motivation is to introduce an intuitive but insightful theoretical framework.

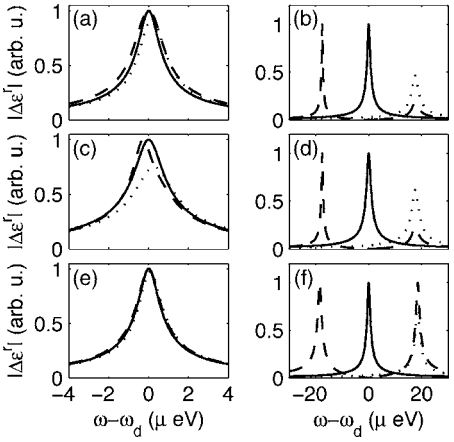

FIG. 1. (a) Single quantum dot (QD) effective permittivity (modulus) for the two-coupled-QD system. The dashed and dotted curves show, respectively, the response for one QD excited and two QD excited incident fields, for dots spatially separated by 100 nm with equal exciton resonance energies; the uncoupled QD calculation is shown by the solid curve. The surface is taken also to be 100 nm from the nearest QD (see text). (b) As in (a) but with a QD separation of 20 nm. (c) As in (a) but for calculations that ignore the effect of the surface. (d) As in (b) but for calculations that ignore the effect of the surface. (e) As in (a) but for calculations that include only the static Förster dipole-dipole interaction. (f) As in (b) but for calculations that include only the static Förster dipole-dipole interaction.

Below we give some representative example calculations by employing the following parameters similar to those of experiments: $\omega_d/(2\pi)\approx 230$ THz, $\Gamma_d=0.5$ μeV, $V_\alpha=V$, and dipole moment $d_\alpha\approx 50$ ($=d_0$) D ($=3.33564\times10^{-30}$ Cm).[4] We also assume that any initial field (if appropriate) on either dot will be identical; note that this is not a model restriction. We consider the situation of two QDs vertically coupled, whose coupling mechanism is primarily (but not exclusively) through the virtual transition of photons; such a process is mathematically described by the real part of, e.g., $\overleftrightarrow{\mathbf{G}}^b(r_a,r_b;\omega)$, which appears in Eq. (3). We point out that such a photon-exchange mechanism is usually ignored or

negligible in coupling atoms or excitons within cavity-QED regimes, but in general photon exchange always takes place through real and virtual photons.

In Fig. 1 we present several example calculations of the single-QD permittivity for two photon-coupled QDs. In Fig. 1(a) we display the renormalized permittivity when the two QDs are separated by R_0 $(=r_a-r_b)=100$ nm, while in Fig. 1(b) the two QDs are separated by $R_0=20$ nm. We plot the absolute value $(|\Delta\epsilon_d^{r2}|)$ as the relevant spectral quantity that will be measured by a photon detector, though the actual quantitative details depend on another GFT propagator—dot to detector—whose specifics need not concern us here (though more details are made clearer in the quantum equations below). For the former case [Fig. 1(a)], which is quite typical for single QD experiments (100 nm separation), we recognize a significant broadening of the lineshape and a resonance shift. In Fig. 1(b), for more closely separated QDs, we obtain a substantial splitting of the QD resonance for one-QD excitation only ($E_b^0=0$, chain curve), even though both QDs have the same exciton resonance; for two-QD excitation (dotted curve), only one peak appears for identical dots with additional energy broadening.

Physically, the extra broadening is a manifestation of superradiance, while the resonance splitting is a measure of the coupling between the QDs. Interestingly, the resonance at the lower-energy side, which is an optically dark state, appears only for one-field excitation; the energy separation of the two peaks also gives a measure of the strength of the photon coupling. The formation of superradiant and subradient states is well known for Dicke states with two identical emitters.[19] The appearance of the optically dark subradiant state here is caused by the nonhomogeneous excitation, whereby the optically dark state can still couple to the light field (see also the discussion in Ref. 16). From a perturbative picture such as Fermi's golden rule, for short distances $(R_0 \sim < \lambda/4)$ the transfer coupling rate $(\propto R^{-6})$ is related to the Förster process, but for longer distances the retarded light-field coupling dominates (transfer rate $\propto R^{-2}$); both contributions are contained within the real part of the GFT given earlier.

For the above simulations we included the effect of a dielectric/air $(\epsilon_b=12/1)$ interface positioned 100 nm above the QDs. We also check to recover the results of other works for point dipoles near interfaces (e.g., Ref. 20) where it is found that the interface distance plays a small role for dielectric/air interfaces less than an optical wavelength but can have a major influence for metal interfaces (not the case for this study). In Figs. 1(c) and 1(d) we repeat the above study with calculations that do not include the interface; while the interface clearly has an influence on the 100-nm-separated QDs, the effect on the 20-nm-separared QDs is much smaller and the dominant effect remains that of photon coupling. Before closing the classical study, we also repeat the calculations with the interface included but only account for static Förster coupling (see, e.g., Eq. (18) in Ref. 18), which are shown in Figs. 1(e) and 1(f). Clearly, both excitation scenarios require a unified treatment that includes retardation in the photon coupling.

III. THE SELF-CONSISTENT QUANTUM-APPROACH

Working again with the photon GFTs one can derive, within a quantum optics picture,[21] the upper-level decay (C_α) of QD α $(\alpha=a,b)$ as

$$\frac{\partial C_\alpha(t)}{\partial t} = -\int_0^t dt' \left(\sum_\beta \mathcal{A}_{r_\alpha r_\beta}(t,t') \right) C_\alpha(t') + \sum_{\beta\neq\alpha} \mathcal{B}_{r_\alpha r_\beta}(t) C_\beta(t), \tag{4}$$

where $\mathcal{A}_{r_\alpha r_\beta}(t,t')=1/(\hbar\pi\epsilon_0)\int d\omega\, e^{i(\omega_\alpha-\omega)t} e^{i(\omega_\beta-\omega)t'} \mathbf{d}_\alpha^* \cdot \mathrm{Im}[\overleftrightarrow{\mathbf{G}}^b(r_\alpha,r_\beta;\omega_\beta)]\cdot\mathbf{d}_\beta$, and $\mathcal{B}_{r_\alpha r_\beta}(t)=i/(\hbar\epsilon_0)\mathbf{d}_\alpha^* \cdot \mathrm{Re}[\overleftrightarrow{\mathbf{G}}^b(r_\alpha,r_\beta;\omega_\beta)]\cdot\mathbf{d}_\beta e^{i(\omega_\beta-\omega_\alpha)t}$. It is worth highlighting that these equations cover both weak- and strong-coupling regimes in terms of the spontaneous emission dynamics and real photon transitions, though we are far from any cavity-QED regimes for our present investigation; but the general formulas can be (and have been) applied to look at, e.g., one and two QDs in strongly coupled cavities.[22,23] Additionally, the first-order quantum correlation function $\langle \mathbf{E}^+(\mathbf{r},t)\cdot\mathbf{E}^-(\mathbf{r},t)\rangle \propto |\Sigma_\alpha[\int_0^t dt' \int_0^\infty d\omega\, C_\alpha(t') \mathrm{Im}\times[\overleftrightarrow{\mathbf{G}}^b(\mathbf{r},r_\alpha;\omega)]\cdot\mathbf{d}_\alpha e^{i(\omega_\alpha-\omega)(t-t')}]|^2$, which accounts for photon detection from QD α to position $\mathbf{r}$. These equations can then be exploited to compute the quantum decay dynamics from any number of coupled QDs by solving the coupled integro-differential equations; the ensuing QD dynamics is initiated only by vacuum fluctuations and depends on the initial wave function of the system. Note that the influence of electron-phonon coupling is neglected here, which is well justified for low temperatures in high-quality samples,[6] especially as we concentrate on the first few hundred picoseconds; the role of phonon scattering for increasing temperatures on single-QD photon decay has been predicted elsewhere[24] and it would be of interest to see how such effects are modified in the presence of photon exchange. We note that quantum corrections due to counter-rotating-wave terms and the homogeneous Lamb shift can in principle be included, but will typically be negligible, and for our purposes can be thought to exist with the (already renormalized) QD resonance ω_α; this is especially true as the frequency dependence of the GFT does not change rapidly over the frequency scales of interest.[21]

The quantum decay dynamics for photon-coupled QDs are presented in Fig. 2, and we first make a connection to the classical results introduced earlier. In Fig. 2(a) is shown the decay dynamics for QDs that are separated by 100 nm, which yield a faster decay for two dots fully excited (dashed curve) than for one QD excited (solid curve), thus yielding superradiance; we also show the decay dynamics for two QDs that have different resonance energies, namely, $\omega_a-\omega_b=0.5$ meV (dotted and chain curves), which demonstrate significant differences in the decay dynamics (these are also phase dependent). We conclude that, in general, one will obtain a nonexponential decay and population transfer to varying degrees that depend on the spatial position and properties of the neighboring QDs and the surrounding environment (GFT). This nonexponential decay is mediated by the dynamics of the hopping photons.

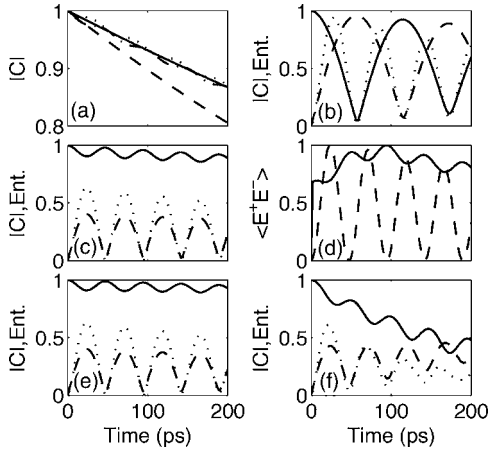

FIG. 2. (a) Quantum dot (QD) upper decay ($|C_i|$) for two dots spatially separated by 100 nm. The solid line is for one QD uncoupled, while the dashed line is for two excited QDs with the same resonance energy. The dotted and chain lines show the decay for two QDs that are detuned (from each other) by 0.5 meV. (b) One QD initially excited with a dot separation of 20 nm; the dot dynamics are shown by the solid and dashed curves, while the entanglement of formation is shown by the dotted curve. (c) As in (b) but for QDs that are detuned by 0.5 meV. (d) Quantum emission dynamics registered on two detectors that monitor the photon emission from the two spectrally different QDs (see text). (e) As in (c) but with the initially excited QD having a 20% larger dipole moment, but the dipole product ($d_1 d_2$) remaining the same. (f) As in (e) but with static Förster dipole-dipole coupling only.

We now consider two QDs separated, as earlier, by only 20 nm. In Fig. 2(b) is displayed the decay dynamics for two QDs for one QD initially excited, and once again [cf. Fig. 1(b)] we obtain a pronounced transfer process; solid and dashed curves show the decay dynamics of both QDs. These quantum solutions are thus consistent with the classical permittivity picture that predicts resonance splitting for one QD excitation. The quantum results in Fig. 2(c) are also significant in the context of quantum information science since they demonstrate that large qubit entanglement between the two QDs is achieved (as evidenced by both populations initially crossing with a value of around $1/\sqrt{2}$—suggesting a mixed Bell state). Labeling our qubits as $|10\rangle$ (QD a excited and QD b in the ground state) and $|01\rangle$ (vice versa), in essence we can create a maximally entangled state when our wave function $|\psi(t>0)\rangle = 2^{-0.5}(|10\rangle \pm |01\rangle)$, whose relaxation can be slower than the one QD decay alone, and is, moreover, phase dependent. While the generation of entangled states via dipole-dipole interaction has been proposed before,[25] this has typically been studied using classical optical fields and (or) unknown coupling parameters (added phenomenologically). Here the approach is significantly more general and self-consistent.

To have a more quantitative measure of how much entanglement is achieved we calculate the concurrence from the reduced density matrix of our two qubits, and then obtain the time-dependent entanglement of formation.[26] The entanglement $E(t)$ as a function of time is also shown in Fig. 2(b) by the dotted curve. Such a large degree of entanglement (>0.9) has been realized without the need for a cavity, and may be used with optical schemes for quantum computation.[18] Clearly we are in a strong-coupling regime, where reversible decay is made possible through QD photon coupling. Importantly, obtaining such a large degree of entanglement from identical QDs and initial conditions (one QD excited in a two-QD system) is impossible to achieve in a high-Q cavity, whose concurrence (entanglement) can never go above 0.5 (0.35 ebits),[27] even in the regime of strong cavity coupling. This is because the entangled solution depends on both the real and imaginary parts of the surrounding environment response. These values cannot be optimized independently as fitting parameters (commonly done in the more phenomenological theories); rather, they must be contained within the GFT that properly describes the entire response of the surrounding medium.

Although such a situation may seem rather obvious for two identical emitters that are very close together, for generally different QDs that are separated by 20 nm or more with different resonant energies and dipole moments, the degree of entanglement is not known and is perhaps not expected to be significant. More realistically, then, we now study the robustness of the entanglement dynamics for different detuning and dipole moments, since in general these will not be identical. Such coupling regimes are thus quite different from studies with identical atoms. First, we detune QD b by 0.5 meV and calculate the resulting emission dynamics and entanglement dynamics, displayed in Fig. 2(c). Although the overall quantum dynamics is certainly more rich, evidently the large degree of entanglement is still obtained; in fact, we still maintain significant degrees of entanglement for detunings of several meV. To probe these entangled dynamics further, we introduce photon detectors D_a and D_b that capture the emission dynamics from QDs a and b (with their different resonance energies) separately, and show the resulting time-dependent quantum emission. Most strikingly, as shown in Fig. 2(d), when a maximum is obtained on detector D_a, then a minimum is obtained on detector D_b; such phenomenon is closely related to antibunching through a second-order correlation measurement.[28]

Next we also change the optical dipole moments of the QDs, and set $d_1 = 0.8 d_2$ but maintain a fixed $d_1 d_2 = d_0^2$ as before. The entanglement dynamics, shown in Fig. 2(e) are still essentially maintained. Such robustness may have advantages over entangling qubits through cavity QED, since the cavity coupling is quickly lost for even minute detunings, and coupling in these homogeneous material systems should be relatively straightforward. However, the problem of electron-phonon coupling that occurs during fast optical pulse control will likely remain a significant problem.[24] Finally, we repeat the calculations and include only the static Förster coupling [see Fig. 2(f)], which yields substantially different (and incorrect) dynamics. Thus we conclude that one must include effects beyond the simple Förster coupling for sufficiently close QDs. Finally we mention that, although the entanglement dynamics oscillates from a maximum to a minumim, which may seem impractical from an applications perspective, the application of an external field can dynamically switch the dipole-dipole coupling off, e.g., through the optical Stark shift. If this perturbation is applied at the cor-

rect timing interval (near a peak), then the large degrees of entanglement can be maintained over a relatively long time scale without any further oscillations.

IV. CONCLUSIONS

In summary, we have presented a nonperturbative light-matter interaction study of photon-coupled single QD excitons in a semiconductor, using both classical and quantum Green function theories for propagating photons. A rich variety of classical and quantum correlation effects are predicted for certain QD configurations, in particular the inhomogeneous excitation of an optically dark resonance and the creation of large degrees of exciton entanglement even for different QDs that are outside the regime of electronic tunneling.

ACKNOWLEDGMENTS

This work was supported by NSERC and CFI, Canada. It is a pleasure to thank A. Knorr for useful discussions.

*Electronic address: shughes@physics.queensu.ca

[1] See, for example, *Quantum coherence, correlation and decoherence in semiconductor nanostructures*, edited by T. Takagahara (Academic Press, New York, 2003).
[2] M. Pelton, C. Santori, J. Vukovi, B. Zhang, G. S. Solomon, J. Plant, and Y. Yamamoto, Phys. Rev. Lett. **89**, 233602 (2002).
[3] P. Chen, C. Piermarocchi, L. J. Sham, D. Gammon, and D. G. Steel, Phys. Rev. B **69**, 075320 (2004).
[4] H. Kamada, H. Gotoh, J. Temmyo, T. Takagahara, and H. Ando, Phys. Rev. Lett. **87**, 246401 (2001).
[5] P. Borri, W. Langbein, S. Schneider, U. Woggon, R. L. Sellin, D. Ouyang, and D. Bimberg, Phys. Rev. Lett. **87**, 157401 (2001).
[6] W. Langbein, P. Borri, U. Woggon, V. Stavarache, D. Reuter, and A. D. Wieck, Phys. Rev. B **70**, 033301 (2004).
[7] G. S. Agarwal, *Quantum Statistical Theories of Spontaneous Emission* (Springer, Berlin, 1974).
[8] P. W. Milloni and P. L. Knight, Phys. Rev. A **10**, 1096 (1974).
[9] G. Kurizki and A. Ben-Reuven, Phys. Rev. A **32**, 2560 (1985).
[10] G. Kurizki, A. G. Kofman, and V. Yudson, Phys. Rev. A **53**, R35 (1996).
[11] S. John and J. Wang, Phys. Rev. B **43**, 12772 (1991).
[12] B. D. Gerardot, S. Strauf, M. J. A. de Dood, A. M. Bychkov, A. Badolato, K. Hennessy, E. L. Hu, D. Bouwmeester, and P. M. Petroff, Phys. Rev. Lett. **95**, 137403 (2005).
[13] See, for example, O. J. F. Martin and N. B. Piller, Phys. Rev. E **58**, 3909 (1998).
[14] See, for example, J. M. Wylie and J. E. Sipe, Phys. Rev. A **30**, 1185 (1984).
[15] A. O. Govorov, Phys. Rev. B **71**, 155323 (2005).
[16] P. Thomas, M. Moller, R. Eichmann, T. Meier, T. Stroucken, and A. Knorr, Phys. Status Solidi B **230**, 25 (2002).
[17] G. Parascandolo and V. Savona, Phys. Rev. B **71**, 045335 (2005).
[18] B. W. Lovett, J. H. Reina, A. Nazir, and G. A. D. Briggs, Phys. Rev. B **68**, 205319 (2003).
[19] R. H. Dicke, Phys. Rev. **93**, 99 (1954).
[20] K. J. Ahn, J. Förstner, and A. Knorr, Phys. Rev. B **71**, 153309 (2005).
[21] See, for example, H. T. Dung, L. Knöll, and D. G. Welsch, Phys. Rev. A **66**, 063810 (2002).
[22] S. Hughes, Opt. Lett. **30**, 1393 (2005).
[23] S. Hughes, Phys. Rev. Lett. **94**, 227402 (2005).
[24] K. J. Ahn, J. Förstner, and A. Knorr, Phys. Rev. B **71**, 153309 (2005).
[25] See, for example, A. Nazir, B. W. Lovett, and G. A. Briggs, Phys. Rev. A **70**, 052301 (2004).
[26] W. K. Wootters, Phys. Rev. Lett. **80**, 2245 (1998).
[27] See, for example, H. T. Dung, S. Scheel, D.-G. Welsch, and L. Knoll, J. Opt. B: Quantum Semiclassical Opt. **4**, 169 (2002).
[28] See, for example, R. Loudon, *The Quantum Theory of Light* (Cambridge University Press, Cambridge, U.K., 1997).